Flaking behaviour of GA IF and GA AHSS and its correlation with the adhesion strength and intefacial residual stress

C. Cheng, V. Krishnardula

Lap Shear test results showed that GA AHSS possess significantly higher adhesion strength than GA IF. SEM examination of the Lap-Shear-tested GA IF specimens revealed adhesive failure at the coating/steel interface with multiple steel grains pulled out from the IF steel substrate. Conversely, SEM results showed all Lap-Shear-tested GA AHSS specimens failed cohesively (failed within the adhesive) and exhibited very little to no GA coating separation from AHSS substrates. A newly developed XRD procedure was used to measure the residual stress on both sides of the coating/steel interface. The gamma layer of GA coating in all GA IF and GA AHSS exhibited a distinct tension residual stress, which matches with theoretical predictions. GA AHSS showed a distinct compressive residual stress on the steel substrate side. However, for most GA IF steels there was no obvious compressive residual stress on the steel substrate side. The lack of compressive residual stress in the GA IF steels is likely due to weakening of the steel grain boundaries by liquid zinc penetration. It is consistent with the Lap Shear test results. Two main differences in the interfacial structure between GA IF and GA AHSS are (a) weak steel grain boundaries likely due to apparent liquid Zn penetration of IF steel grain boundaries and (b) relatively smoother coating/steel interface of GA IF. These two factors contribute significantly to the poor flaking resistance of GA IF.

Keywords:
Lap Shear Test, Liquid Zn Penetration, Adhesive Failure, Cohesive Failure, XRD

INTRODUCTION

During stamping of galvannealed (GA) steel sheets, one of the major failure modes is flaking. It is widely known that, other than non-optimal stamping die settings and conditions, the presence of a thick gamma layer at the coating/steel interface plays a crucial role in the flaking mechanism [1, 2]. In authors' experience, GA Interstitial-Free (IF) steel with a gamma layer thicker than 1.2 μm has a high affinity for flaking at stamping plants. Fig. 1 shows the relationship between the gamma layer thickness and severe flaking issue in 484 actual working samples from customers' stamping plants over a period of about three years. The majority of the 484 samples in Fig. 1 were processed within the optimal die conditions and settings. Only a few, predominately samples with thinner than 1.0 μm gamma, were processed with non-optimal die conditions and settings. The data clearly showed that when the gamma layer thickness in GA IF exceeded 1.2 μm, the flaking complaints and rejections were higher than 50%. Fig. 2 (a) illustrates the appearance of a stamped sample that suffered severe flaking issue and Fig. 2 (b) shows the separation of GA coating from the gamma/steel interface in the defect areas.

Recently, GA Advanced High Strength Steels (AHSS) has become one of the key improvements for lightweight and better-fuel-efficiency vehicle applications. Some of the GA AHSS under development are intended for exposed automotive body applications. GA AHSS, in contrast to GA IF steels, rarely fails by flaking mode, even when the gamma layer thickness is greater than 1.5

C. Cheng and V. Krishnardula
ArcelorMittal Global R&D
East Chicago, IN 46312 USA

Paper presented at the 8th Int. Conf. GALVATECH 2011, Genova, 21-25 June 2011

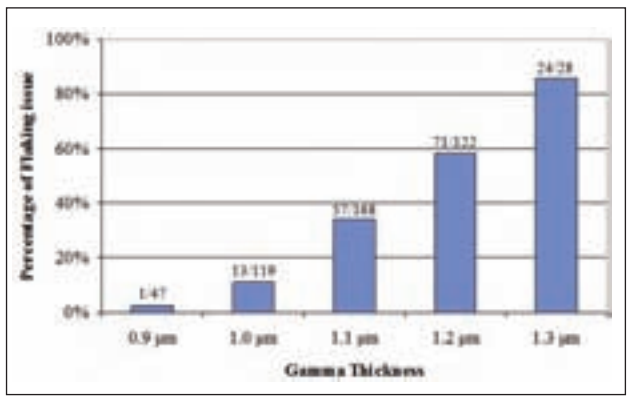

FIG. 1 ***Percentage of flaking issue versus measured gamma thickness in total 484 GA IF exposed samples from customers. The ratios above the bars are the actual numbers of flaking issue samples to the total received samples of the investigation.***

Percentuale di sfogliatura versus spessore gamma misurato su un totale di 484 reperti difettosi di acciaio GA-IF inviati da clienti dopo lavorazione. I rapporti sopra le barre indicano il numero di reperti con una data entità di sfogliatura rispetto al numero totale di reperti ricevuti.

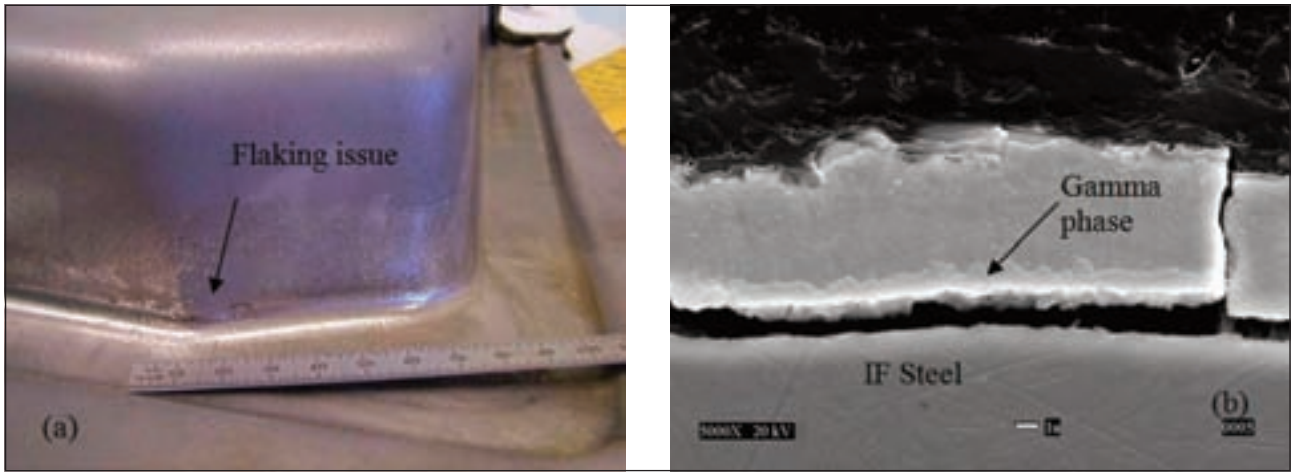

FIG. 2 ***(a) Appearance of flaking failure on a formed part. (b) Cross-sectional SEM view of the flaking failure area showing GA coating delamination at the gamma/steel interface.***

(a) Aspetto del difetto di sfogliatura su un materiale stampato. (b) Vista della sezione trasversale al SEM dell' area del difetto che mostra la delaminazione del rivestimento di zincatura all'interfaccia gamma/acciaio.

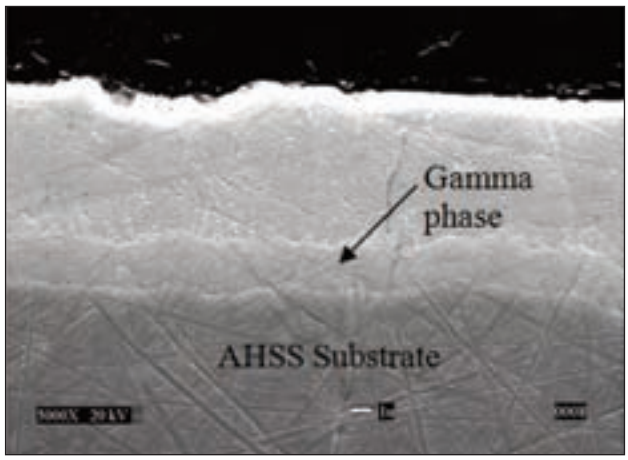

FIG. 3 ***GA coating with a gamma layer thicker than 1.5 µm on AHSS substrate with no flaking issue.***

Rivestimento di zincatura con uno strato gamma di spessore superiore a 1.5 µm su substrato di acciaio GA-AHSS senza sfogliature.

µm, as shown in Fig. 3 of a GA Dual Phase (DP) sample. According to authors' experience, the flaking issue seems to be one of the unique characteristics of GA IF and rarely occurs in GA AHSS materials. Fundamentally, flaking failure appears to be a result of the coating/steel interfacial separation and is influenced by factors such as interface structure, adhesion strength, and interfacial residual stress. There are several major differences in the coating/steel interface in GA IF and GA AHSS materials that lead to different flaking resistance behavior of both materials.

Interfacial adhesion strength generally can be directly measured by the Lap Shear test. However, the Lap Shear test by itself has its own complications, such as types of adhesive, thicknesses and uniformity of adhesive layer, with or without backing plate, and bonding area size that could affect the end results [3]. In addition, most previous adhesion strength measurements by the Lap Shear tests were conducted on the IF based substrates [3, 4] and rarely on AHSS substrates. In literature, the GA IF steels typically exhibited adhesion strengths of 20 MPa or lower, which is below the general requirement for adhesive bonding application as set by the automotive manufacturers. A recent joint adhesive bonding project [5, 6] between ArcelorMittal USA Global R&D and Dow Chemical Company aimed to evaluate the feasibility of adhesive bonding application on GA products. The project included both GA IF and GA AHSS materials for automotive body applications. In the past, Lap Shear tests suggested that GA product is not suitable for adhesive bonding application. This perception was primarily based on GA IF steels. The Lap Shear test results [5, 6] from the above joint study showed a different view of the adhesive bonding application using GA materials. It indicated that adhesive bonding application is dependent on the steel substrate and not necessarily dependent on the GA coating. The results indicated that adhesive bonding was not suitable for GA IF steels. However, acceptable adhesive bond strengths were achieved using GA AHSS. One major difference in the Lap Shear test results between GA IF and GA AHSS is the fracture failure location. All AHSS materials failed cohesively i.e., within the adhesive. On the contrary, all GA IF materials failed adhesively at the gamma/steel interface. Interfacial strength, structure, and residual stress could be key factors to explain the differences in the fracture behavior (flaking resistance) of the GA materials.

Residual stress at the coating/steel interface is a result of lattice mismatch and a product of different thermal expansion between the coating and the substrate. In general, the presence of residual stress is considered to be an indicator of the nature and degree of bonding at the interface. Theoretically, if residual stress is present at the interface, opposite forces should be present on both sides of the interface. For example, the substrate may contain compressive stress and the coating may contain tension stress or vice-versa. Typically, the former combination of stresses is considered to be beneficial to the coating adhesion [7, 8]. Among several techniques, X-Ray Diffraction (XRD) is one of the most common and direct techniques to measure residual stress. However, for years, it was considered to be extremely difficult, if not impossible, to measure residual stress in a GA system [9]. No experimental data was available in the literature on residual stress measurement in a GA system. Only limited work on theoretical modelling was available [10, 11]. In this study, a newly developed XRD technique with a Parallel Beam optics was used successfully to measure the residual stress, not only on the coa-

ting side (gamma layer) of GA IF and GA AHSS materials, but also on the steel substrate side immediately adjacent to the coating/steel interface. These are possibly the first experimental residual stress results reported for any GA products.
In this study, we extract Lap Shear test results from our previous adhesive bonding study to show the difference in the fracture failure mode of GA IF and GA AHSS materials. Top-view SEM observation was conducted on stripped and lightly etched steel substrates. The observations revealed the differences in steel grain structure, interface roughness of both materials, and possible liquid Zn penetration along the steel grain boundaries of IF material. XRD residual stress measurements showed that there is a distinct tension stress on the gamma layer of all GA IF and GA AHSS materials, which is consistent with theoretical models [10, 11]. A distinct compressive residual stress is seen on the GA AHSS steel substrate. On the contrary, most GA IF steel substrates did not possess obvious compressive residual stress. Cracks and imperfections in the steel grain boundaries can lead to the lack of compressive residual stresses. IF steel surface exhibited wider grain boundaries than the AHSS that can contribute to the lack of compressive residual stresses. It is possible that liquid zinc penetration resulted in wider steel grain boundaries in IF steels.

MATERIALS AND EXPERIMENTAL PROCEDURES

Materials and Lap Shear Test

GA IF material used in this study is Ti-Nb dual stabilized IF steel. GA AHSS materials include DP590, TRIP590, 590R (complex phase, high yield to tensile ratio), DP780, and TRIP780. Their steel chemistries, GA coating chemistries and other properties can be found in the two original SAE papers [5, 6]. Crash durable adhesives used in this study were developed by Dow Chemical Company. The adhesive is designed not only to absorb impact energy but also to effectively transfer a portion of the energy into the metal component so that it can plastically deform. Both Betamate 1496 and 1488 adhesives have a lower modulus, 1600 MPa and 1400 MPa respectively, compared to conventional hem flanging adhesives, typically with a high modulus of about 3500 MPa. The bonding surface of the GA steel strips, around 12.7 mm (0.5") along the strip length, was cleaned with acetone, then a light coating of Ferrocote 61AUS oil was applied. The adhesives to be evaluated were applied to each strip and two strips were bonded together to form a lap shear joint with an overlap of 12.7 mm (0.5"). The bond thickness was controlled at 0.25 mm using glass beads sprinkled in the adhesive. The bonds were kept together with clips and placed in an oven set at 180°C for thirty minutes to cure the adhesive. After cooling, the samples were pulled on an Instron tensile tester at a rate of 12.5 mm/min. Load and displacements were recorded. The detailed procedure of the Lap Shear test can be found in references 5 and 6.

Residual Stress Measurement by XRD

A PANalytical X'Pert PRO X-Ray Diffractometer with a Co radiation source along with its stress software is used in this study. A thorough development of the theory of XRD residual stress measurement can be found in the SAE publication [12]. However, in simpler terms without complicated mathematics, it can be explained as follows: residual stress is an extrinsic property and must be calculated from a directly measurable property such as strain, or force and area. In the XRD method, the strain is measured in crystal lattice d-spacing, and the residual stress producing the strain is calculated assuming a linear elastic distortion of the crystal lattice. Because the elastic strain changes the mean lattice spacing, the elastic strains are measured by XRD. When the elastic limit of the subject materials is exceeded, further strain results in cracks in the coating, coating delamination from the substrate, and failure. Equation (1) expresses the fundamental relationship between lattice spacing and the residual stress at the interface of the sample [12]. The change of lattice spacing is a linear function of $\sin^2 \psi$ and the residual stress (σ) can be determined from the slope of the lattice spacing vs. $\sin^2 \psi$ plot.

$$\Delta d \sim [(1+\nu)/E] \times \sin^2 \psi \times \sigma \qquad (1)$$

Δd: Change in lattice spacing (Å)
σ: Residual stress (MPa)
ψ: Tilting angle (°)
ν: Poisson Ratio
E: Modulus of Elasticity (GPa)

Another way to interpret the physical meaning of equation (1) is when the tilting angle, ψ, is zero; the d-spacing measured by XRD is a stress-free lattice d-spacing because the direction of residual stress is parallel to the set of lattice plane. When the tilting angle is not zero, there is always a stress component that is perpendicular to the set of plane and therefore affects the lattice d-spacing. The Fe 211 peak and gamma 721 peak are used in this study for the residual stress measurement on steel substrate and gamma layer, respectively. The residual stress determined using XRD is the arithmetic average stress in a volume of material defined by the irradiated area. For steel substrate, in this study, it is the area about 30 μm deep from the GA coating/steel interface. Accurate and precise measurement of dif-

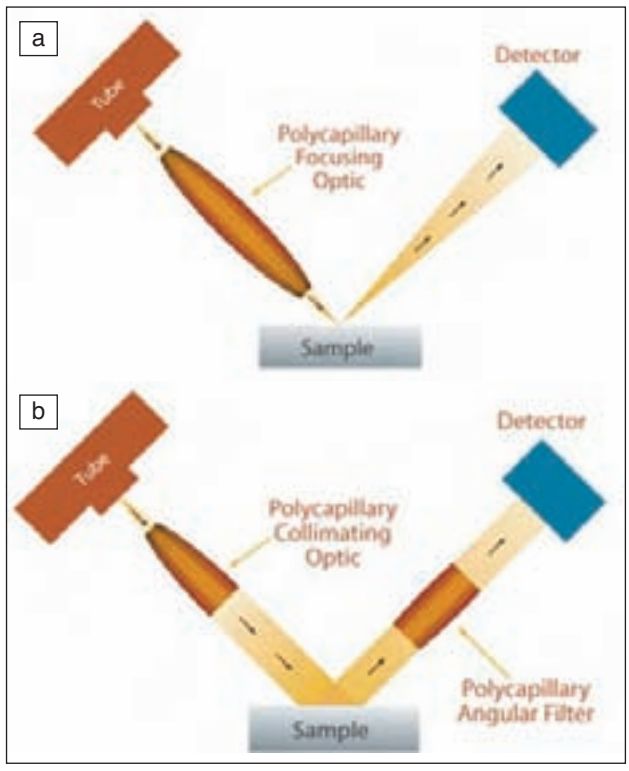

FIG. 4 ***The schematic diagrams of (a) the conventional Bragg-Brentano optics and (b) the Parallel Beam optics (X-ray beam size is not in scale).***

Diagrammi schematici di (a) esame Bragg-Brentano con ottica convenzionale e (b) esame con ottica a Fasci Paralleli (la dimensione del fascio di raggi X non è in scala).

TABLE 1
XRD residual stress measurement parameters.
Parametri delle misure XRD delle tensioni residue.

Phase	Peak ID	Peak Position	Scanning Range
Steel	211	99.699°	97.5° to 101.5°
Coating Gamma	721	94.350°	92.0° to 96.0°
Tilting Angles	±33.211° ($\sin^2\psi = 0.3$), ±26.565° ($\sin^2\psi = 0.2$), and ±18.435° ($\sin^2\psi = 0.1$)		

TABLE 2
First set of the Lap Shear test results.
Prima serie di risultati delle prove di taglio per trazione.

Steel	Lap Shear test Load, MPa (with 1.6 mm backing plate)	
	With Betamate 73305GB (high modulus, 3500 MPa)	With Betamate 1496 (low modulus, 1600 MPa)
EDDS-IF (0.8 mm)	20 ± 1.4 (100% AF*)	18 ± 2.6 (100% AF)
DP780 (1.1 mm)	40 ± 1.5 (100% CF**)	32 ± 1.2 (100% CF)
TRIP780 (1.0 mm)	42 ± 1.7 (100% CF)	36 ± 3.4 (100% CF)

*AF: Adhesive Failure, fail at the interface.
**CF: Cohesive Failure, fail inside the adhesive.

TABLE 3
Second set of the Lap Shear test results.
Seconda serie di risultati delle prove di taglio per trazione.

Steel	Lap Shear test Load, MPa (with Betamate 1488, low modulus, 1400 MPa)	
	With 1.6 mm backing plate	Without backing plate
EDDS-IF (0.7 mm)	28 ± 1.0 (100% AF*)	14 ± 0.4 (100% AF)
DP590 (0.7 mm)	31 ± 1.3 (100% CF**)	24 ± 0.5 (99% CF)
TRIP590 (1.5 mm)	32 ± 1.0 (100% CF)	30 ± 0.8 (99% CF)
590R (1.5 mm)	35 ± 0.9 (100% CF)	32 ± 0.8 (100% CF)

*AF: Adhesive Failure, fail at the interface.
**CF: Cohesive Failure, fail inside the adhesive.

fracted peak positions from a sample surface is a non-trivial task in residual stress studies. Hence, in this study, the XRD residual stress measurement utilizes the Parallel Beam optics, instead of the conventional Bragg-Brentano optics. The advantage of Parallel Beam XRD technique [13, 14] is the insensitivity to (a) sample geometry and (b) displacement errors, both of which in most cases lead to asymmetric peak broadening and inaccurate peak positions. This is especially important for very rough interface which is the case for GA AHSS materials. Parallel Beam optics also provides more homogenous energy distribution within the optics and higher beam intensity for deeper penetration. This is particularly important when the measurements require high degrees of tilting. Fig. 4 illustrates the difference between the conventional Bragg-Brentano optics and the Parallel Beam optics. The Bragg-Brentano optics uses a line X-ray source and the Parallel Beam optics uses a point X-ray source, which is smaller than a line source (not in scale as shown in Fig. 4). In fact, attempts of using the conventional Bragg-Brentano optics to measure the residual stress in GA systems failed due to severe peak broadening and insufficient peak intensity. Parallel Beam optics includes a point Co radiation source, a poly-capillary lens in the incident beam path, and a parallel plate collimator as well as a proportional detector in the diffracted beam path. XRD residual stress measurement parameters used in the present study are given in Table 1. Three titling angles on both directions were used for both steel and gamma layer measurements. Each residual stress measurement included 14 scans (7 scans were along the rolling direction and 7 scans were perpendicular to the rolling direction). The peak positions were then fitted by the Centered Center Gravity method [15]. The residual stress of the sample was determined by the slope of d-spacing vs. $\sin^2\psi$ plot. The Poisson's ratio and Young's Modulus for steel and gamma used in this study are 0.30, 223 GPa and 0.25, 209 GPa, respectively.

RESULTS AND DISCUSSIONS

Table 2 and Table 3 show the Lap Shear test results adapted from the author's previous project. Each data point was the average of ten Lap Shear tests. The most noticeable finding from these tests is the predominant fracture failure in the GA IF steels at the coating gamma/steel interface versus fracture failure in the GA AHSS in the Betamate adhesive. Therefore, the results in Table 2 and Table 3 are indicative of coating adhesion strength in GA IF and Betamate adhesive strength in GA AHSS. For example,

FIG. 5
(a) Steel side of the fractured GA IF specimen exhibiting several steel grains pulled out from the substrate surface. (b) GA coating side exhibiting attached several steel grains. Insert is showing EDS spectrum identifying steel grains.

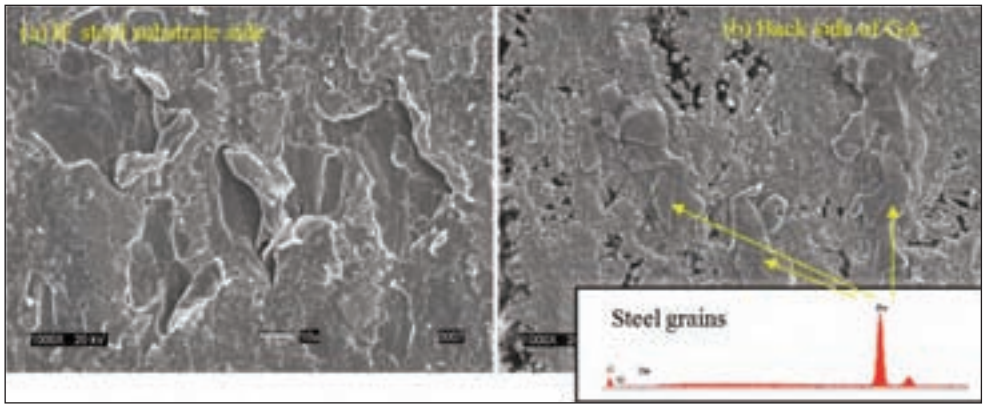

(a) lato acciaio del provino di GA-IF che mostra diversi grani di acciaio strappati dalla superficie del substrato. (b) lato del rivestimento di zincatura che mostra diversi grani di acciaio rimasti attaccati;l'inserto mostra lo spettro EDS che identifica i grani di acciaio.

FIG. 6
(a) – (d) show cross-sectional views of multiple GA IF specimens that were partially Lap-Shear tested.

(a) – (d) mostrano sezioni trasversali di diversi provini di acciaio GA-IF che sono stati sottoposti a prove di taglio per trazione.

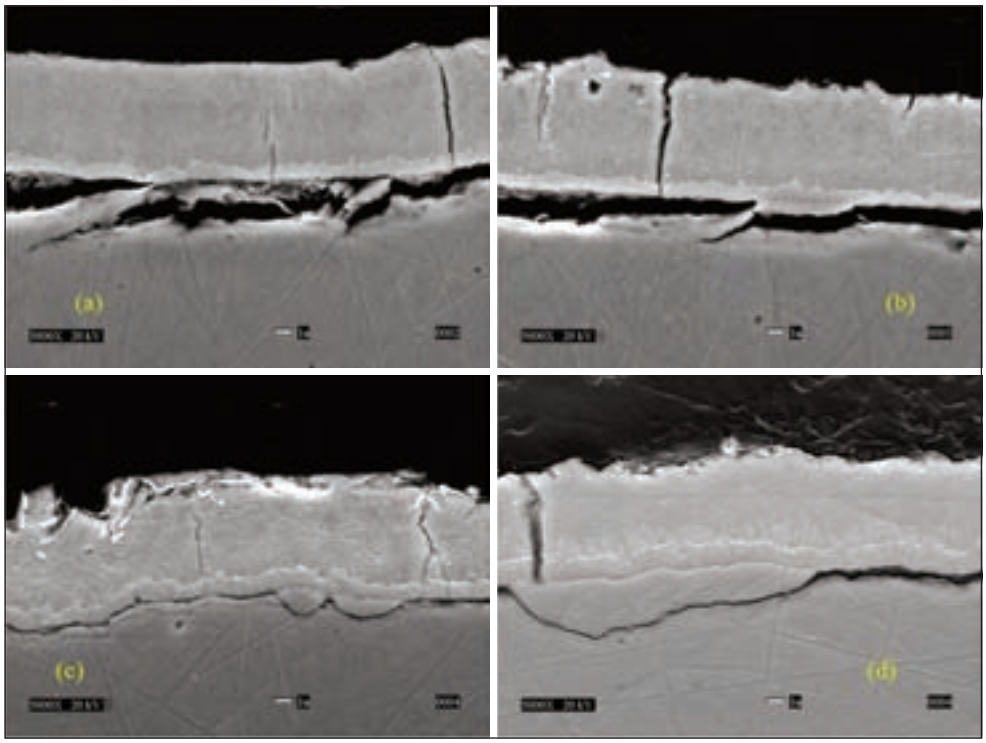

although GA TRIP780 has higher Lap Shear strength than that of GA DP780 in Table 2, it is incorrect to conclude that GA TRIP780 has stronger coating adhesion strength than GA DP780. Similarly, in Table 3, the coating adhesion strength of GA 590R is not necessarily stronger than GA DP590 and GA TRIP590. Overall, GA AHSS have higher coating adhesion strength than GA IF steels. This observation clearly indicates that the interface structure of GA IF is inferior to that of GA AHSS.

The Lap-Shear-tested GA IF specimens were examined by SEM. Fig. 5 shows the steel substrate side and the GA coating side of the fractured test specimen, which revealed that several steel grains were pulled from the steel substrate surface and adhered to the coating gamma layer. In the literature [3, 16], steel grain separation was reported as a result of liquid Zn penetration that leads to weak grain boundary strength of steel substrate. In order to evaluate the fracture development, limited interrupted Lap Shear tests were conducted, in which the test was stopped before the complete fracture of the specimen. Cross-sectional examination of these interrupted test specimens provided additional evidence that steel grains separated from the substrate and adhered to the coating gamma phase. Fig. 6 shows that the initial separation occurred not only at the gamma/steel interface, but also within the steel grains, preferably grain boundaries that were weakened by the liquid Zn. It suggests that weak steel grain boundary may be a major contributor to the poor adhesion strength and flaking resistance of GA IF system.

Residual stress levels in the natural state of the interface region were investigated for both GA IF and GA AHSS systems using the new XRD technique. Each sample was measured at least five times at different locations and the results are given in Table 4. A stress value range was obtained for each sample. The ranges of measured residual stress in this study are generally within a similar range, except that of the GA IF steel. A theoretical model predicted that the residual tension stress in the GA coating is affected by the presence and density of cracks that occur naturally in the GA coating [10]. These cracks are likely a result of thermal expansion variation between the steel substrate and the coating. Smaller crack spacing was reported to yield lower residual stress in the GA coating. These cracks occur randomly and difficult to characterize in terms of crack density and crack orientation.

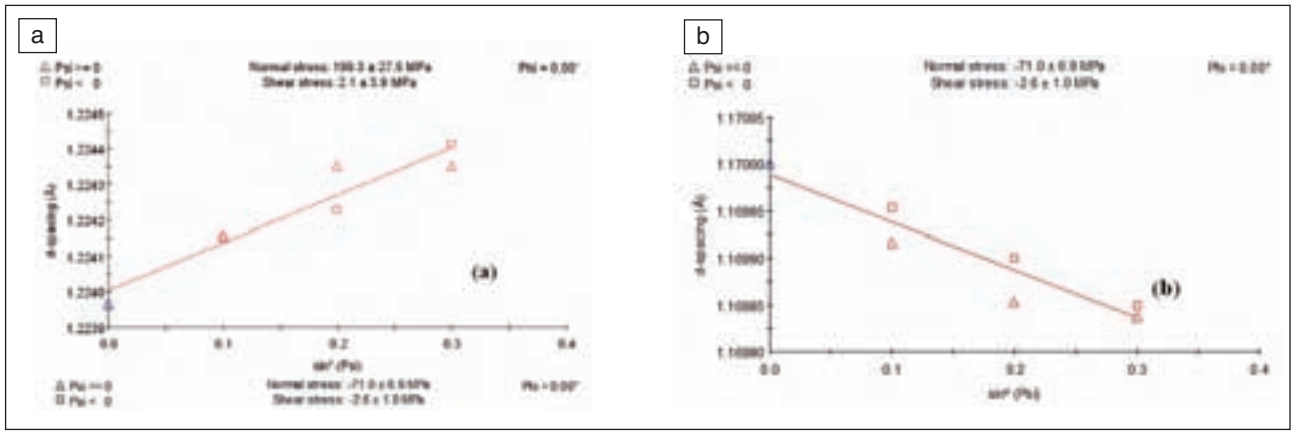

FIG. 7 ***Residual stress measurement of GA DP by XRD. (a) Stress plot for the gamma layer, (b) stress plot for the steel substrate.***

Misure delle tensioni residue degli acciai GA-DP mediante XRD. (a) tracciato della tensione per lo strato gamma, (b) tracciato della tensione per il substrato di acciaio.

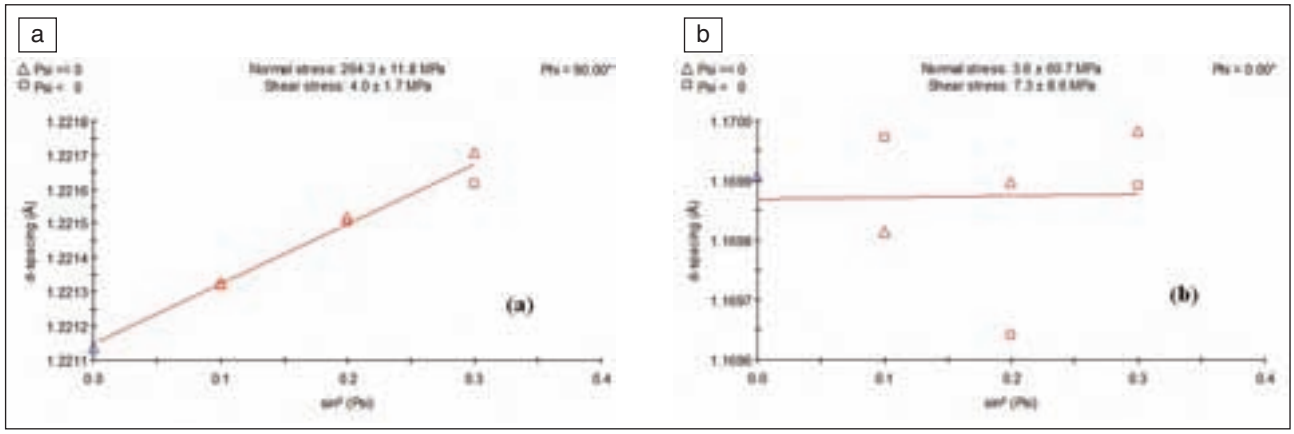

FIG. 8 ***Residual stress measurement of GA IF by XRD. (a) Stress plot for the gamma layer, (b) stress plot for the steel substrate.***

Misure delle tensioni residue degli acciai GA-IF mediante XRD. (a) tracciato della tensione per lo strato gamma, (b) tracciato della tensione per il substrato di acciaio.

The depth of X-ray beam penetration was estimated using the Mass-Absorption-Calculator (MAC) from the PANalytical HighScore Plus software. The penetration was from the coating surface up to ~30 μm deep into the steel substrate. For measuring the stress on the gamma layer, the minimum gamma thickness is learned to be at least 1.1 to 1.2 μm, which suggests that typical GA products that have a gamma layer thinner than 1.0 μm may not be suitable for the stress measurement on the gamma phase. The gamma peak 721 at 94.350° becomes too weak and too broad when the gamma layer is too thin (≤1.0 μm). Fig. 7 and Fig. 8 are the plots of residual stress measurements for GA DP and GA IF materials.

Table 4 shows there is a distinct tension residual stress on the gamma layer of all specimens. The theoretical model estimated that, assuming there was no crack in the coating, the residual stress on the GA coating, presumably on the gamma phase, was around 260 to 270 MPa [10, 11]. This theoretical calculation result appears to be very close to the high ends of our experimental result with the presence of cracks in the coating. Table 4 also indicates that there is a distinct compressive residual stress on the steel substrate, except GA IF material. Measurements conducted on more than ten different GA IF materials with different Fe% in the coating (from about 8% to 14%), steel thickness (from 0.7 mm to 1.6 mm) and with/without temper rolling treatment indicated about 80% of GA IF substrates possess no or near zero residual stress on the steel substrate.

The zero stress results in GA IF can be explained as follows; typically at the steel/coating interface, the steel substrate and the coating possess a compressive stress and a tensile stress, respectively. However, liquid zinc grain boundary penetration into the steel substrate leads to the separation of the grains and hence, contributes to stress relaxation in the substrate. This XRD residual stress finding seems to support that the IF steel substrate exhibits no stress is likely due to the presence of cracks that were caused by the liquid Zn penetration. Whereas in GA AHSS XRD results showed compressive stresses, as there is no Zn penetration and no stress relaxation. Traditional perception on poor flaking resistance of GA products was learned primarily from GA IF materials. Among all GA materials, GA IF is only an exception of GA products that has dubious steel grain structure that is vulnerable to Zn penetration and weakened steel grain boundaries. IF steels have excellent formability and drawability due to its very clean grain boundaries. During the hot dipping process, the IF steel surface grain boundaries are incli-

TABLE 4
Residual stress measurements of GA IF and GA AHSS by XRD.
Misure delle tensioni residue degli acciai GA-IF e GA-AHSS mediante XRD.

Steel	Residual Stress* (MPa)	
	On Gamma layer	On steel substrate (~30 µm penetration depth)
EDDS-IF (0.8 mm)	+120 to +265	~ +10 to -50
DP780 (1.1 mm)	+190 to +260	-50 to -90
TRIP780 (1.0 mm)	+180 to +210	-50 to -160
DP590 (1.6 mm)	+160 to +210	-30 to -60
TRIP590 (1.6 mm)	+160 to +200	-50 to -80
590R (1.5 mm)	+170 to +200	-50 to -80
*at least five measurements per each sample.		

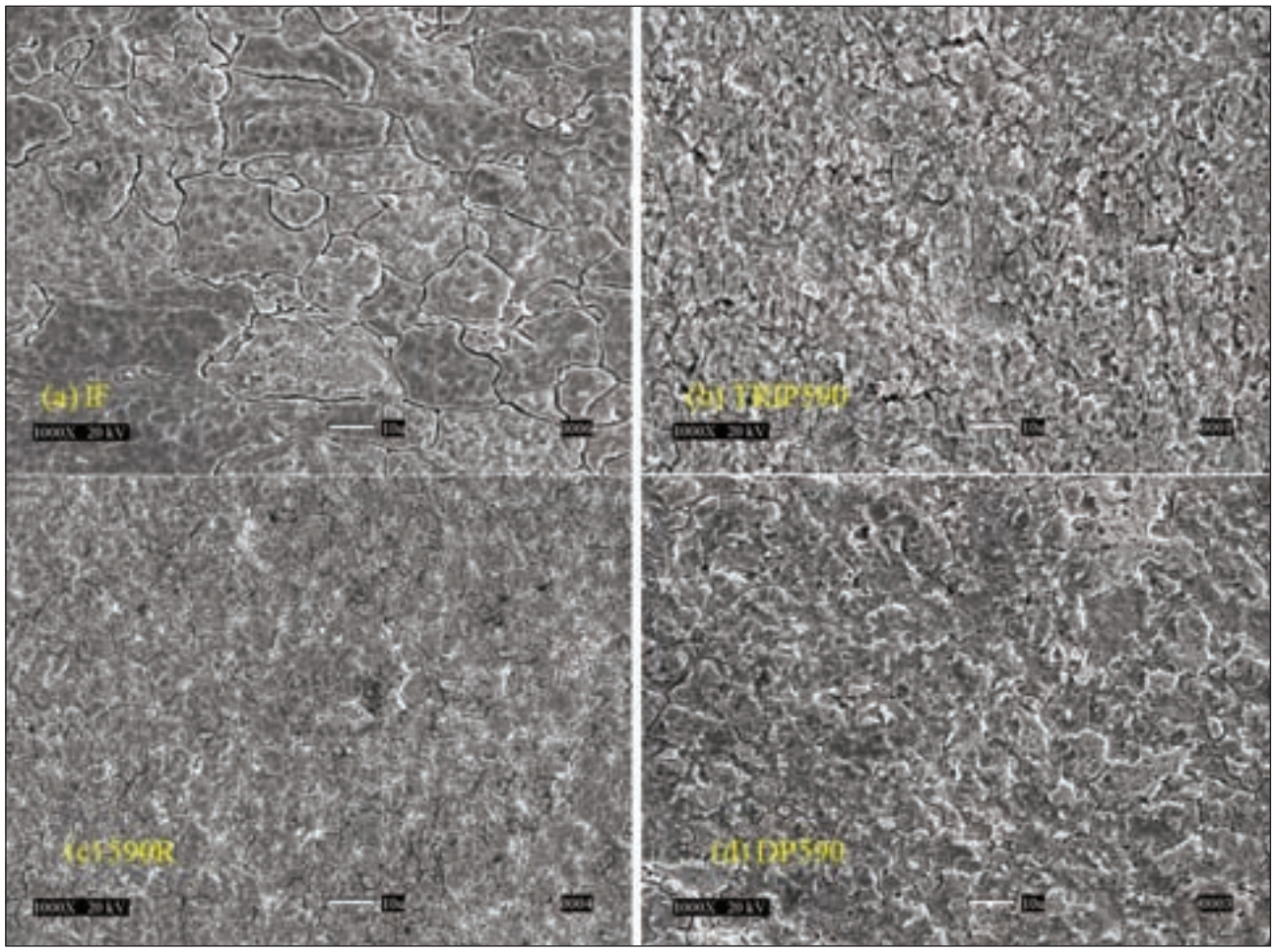

FIG. 9 ***Steel grain and grain boundary structure of the stripped and lightly etched steel surfaces (original GA/steel interface) of (a) GA IF, (b) GA TRIP590, (c) GA 590R, and (d) GA DP590.***
Microstruttura dei grani di acciaio e dei bordi di grano appartenenti alle superfici di acciaio sottoposte a stripping e a leggero attacco chimico (acciaio GA originale /interfaccia acciaio) di (a) GA-IF, (b) GA-TRIP590, (c) GA-590R, e (d) GA-DP590.

ned to be weakened by the liquid zinc penetration [3, 16]. The difference between AHSS steels and IF steels is that AHSS steels have many added alloying elements, like Mn, Si, P, and, Al. During the annealing stage of the galvanizing/galvannealing processes, those alloying elements have a high tendency of segregating and occupying grain boundaries. The segregation of

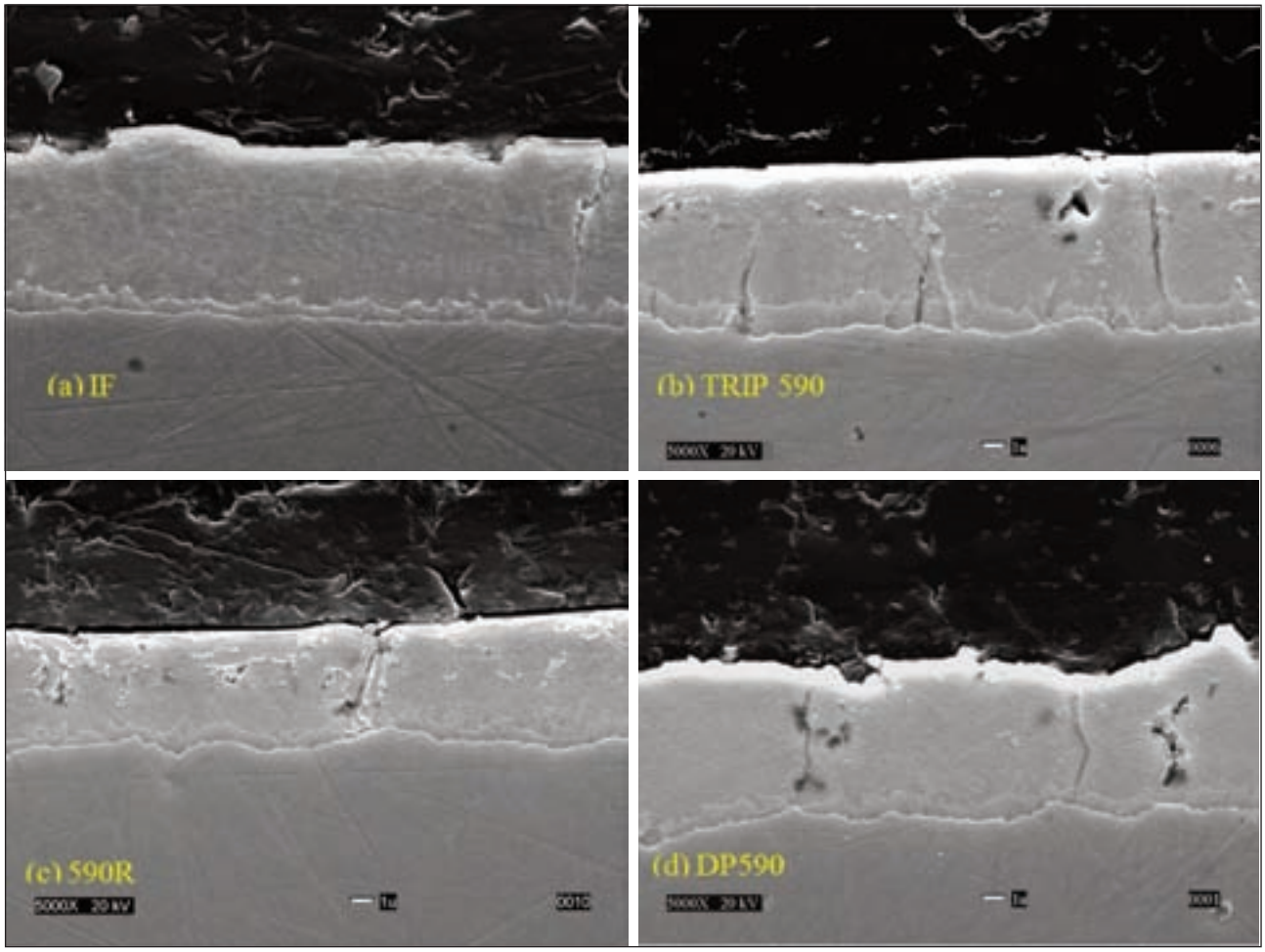

FIG. 10 ***Cross-sectional views of as-received (a) GA IF, (b) GA TRIP590, (c) GA 590R, and (d) GA DP590.***
Sezioni trasversali di materiale as-received di acciaio (a) GA-IF, (b) GA-TRIP590, (c) GA-590R, e (d) GA-DP590.

alloying elements to steel grain boundaries and steel surface generally reduces the wettability of liquid Zn on steel surface and creates process difficulties. On the other hand, segregation of alloying elements to grain boundaries and steel surfaces prohibits liquid Zn penetration and hence enhances the strength of the steel sub-grains that are just below the GA coating.
Besides Zn penetration that leads to crack formation in IF steel grain boundaries, we also found there are differences in interface structure and morphology between GA IF and GA AHSS. Fig. 9 show the stripped and lightly etched (by 4% Nital) steel substrates of GA IF and GA AHSS (GA DP590, GA TRIP590, and GA 590R). Three obvious differences between GA IF and GA AHSS can be observed: 1) the steel grain size is much larger in GA IF than that of GA AHSS, 2) the roughness of the steel surface (which is the original interface) is much smoother in GA IF than that of GA AHSS, and 3) the steel grain boundaries are much wider in GA IF than that in GA AHSS. The unusual wider steel grain boundaries of the GA IF sample, as shown in Fig. 9 (a), seems to allude the original presence of liquid Zn penetration in GA IF materials. Fig. 10 are the cross-sectional views of the same four as-received materials. It clearly shows the relatively rougher interface of GA AHSS than that of GA IF.

CONCLUSIONS

Flaking resistance of GA IF materials was Lap Shear tested along with GA AHSS (DP780, TRIP780, DP590, TRIP590, and 590R). Lap Shear test results showed significantly weaker adhesion strength of GA IF materials than that of GA AHSS. More importantly, GA IF materials suffered 100% adhesive failure i.e., failed at the GA/steel interface. All GA AHSS materials failed cohesively i.e., failed within the adhesive, while the GA/steel interfaces were mostly intact. After examining GA IF tested pieces, many pulled-out steel grains were observed attaching to the back side of GA coating. It suggests that the IF steel grain boundaries were weakened, possibly by liquid Zn penetration during the hot dipping process. Weak steel substrate surface (with liquid Zn penetration) may be the primary culprit for poor flaking resistance of GA IF materials.
Residual stress measurements by X-Ray Diffraction technique was used to reveal the force balancing at the GA/steel interface of GA IF and GA AHSS. All GA samples were measured to have a distinct tension stress on the gamma layer from +120 to +265 MPa, which is consistent with theoretical models prediction in the literature. The wide range of tension stress is due to the crack formation and crack presence inside the GA coating. Theoretical models showed that the density and direction of cracks in the coating can significantly affect the magnitude of the residual stress at the interface. On the other hand, all GA AHSS materials were measured to have a distinct compressive stress on the steel substrate. However, no obvious stress was observed on the steel substrate side of most GA IF samples. Steel grain boundary cracking of GA IF materials due to liquid Zn penetration is believed to be the reason for no or near zero compressive stress in IF steel substrate.

Besides steel grain boundary cracking, relatively smoother GA/steel interface and larger steel grain size are also the possible attributing factors of the weak flaking resistance of GA IF materials. Traditional perception was that GA/steel interface is weak and GA products tend to suffer severe flaking issue during stamping process when the gamma layer is thick, >1.2 μm. This study shows that the weak flaking resistance is a character unique only to GA IF materials. Most other GA products, especially GA AHSS, do not suffer flaking issue easily.

ACKNOWLEDGEMENTS

The authors gratefully acknowledge Mr. Warren Bolton for his masterful metallographic work on preparing cross-sectional micros. The permission for the publication of this report is acknowledged to ArcelorMittal Global R&D management.

REFERENCES

1) C. Cheng, V. Rangarajan, L. Franks, and J. L'Ecuyer, GalvaTech 1992, CRM, P. 122-126.
2) V. Jagannathan, GalvaTech 1992, CRM, p. 127-131.
3) K. Meseure, and et al, ISIJ Intl., V.39, p.1280-1288 (1999).
4) C. Lin ands Meshii, Metallurgical and Materials Transactions B, Vol. 25B, No. 10, p. 721 (1994).
5) J. Bandekar, and et. al., SAE Technical Paper 2010-01-0434.
6) S. Wolf, and et. al., SAE Technical Paper 2011-01-1052.
7) J. Sundgren and H. Hentzell, J. Vac. Sci. Technol., Vol. A4, pp. 2259-2279.
8) B. Bhushan and B. Gupta, "Handbook of Tribology; Materials, Coatings, and Surface Treatments" 1991 by McGraw-Hill, Inc., pp 15.39-15.45.
9) A. Iost and J. Foct, J. of Mater. Sci. Let., V. 12, p.1340-1343 (1993)
10) S. Ochiai and el al., Tetsu-to-Hagane, V. 91, #3, p. 327-334 (2005)
11) S. Iwamoto, and el. Al., ISIJ Intl., V. 47, No. 6, p. 930-934 (2007)
12) A. Ahmad, P. Prevey, and C. Rudd, Residual Stress Measurement by X-Ray Diffraction", SAE HS-784, 2003 Edition, SAE International.
13) T. Watkins, O. Cavin, J. Bai, and J. Chediak, JCPDS-International Centre for Diffraction Data 2003, P. 119-129.
14) Y. Yan and W. Gibson, JCPDS-International Centre for Diffraction Data 2002, P. 298-305.
15) V. Hauk and E. Macherauch, Adv. In X-ray Anal., V. 27, p. 81-99.
16) Y. Hisamatsu, International Conference on Zn and Zn Alloyed Coated Steel Sheet, GalvaTech'89, 1989, pp.3-12.

Abstract

Comportamento a sfogliatura di acciai zincati GA-IF e GA-AHSS e correlazione con la forza di adesione e tensione residua interfacciale

Parole chiave: acciaio inossidabile – rivestimenti

I risultati delle prove di taglio per trazione hanno dimostrato che gli acciai GA-AHSS (GalvAnnealed Advanced High Strength Steels), zincati, hanno una forza di adesione significativamente superiore rispetto agli acciai GA-IF (GalvAnnealed Interstitial-Free), zincati. Gli esami SEM condotti su campioni di GA-IF sottoposti a prove di taglio per trazione hanno rivelato distacco all'interfaccia rivestimento/acciaio con diversi grani dell' acciaio strappati dal substrato di acciaio IF. Al contrario, i risultati delle analisi SEM hanno mostrato che tutti i provini di GA-AHSS sottoposti a prove di taglio per trazione hanno subito distacchi coesivi (rotture entro il rivestimento) e non hanno subito alcuna (o al più molto ridotta) separazione del rivestimento GA dall'acciaio AHSS del substrato. Una procedura XRD di nuova concezione è stata usata per misurare la tensione residua su entrambi i lati dell'interfaccia rivestimento/acciaio. Lo strato gamma del rivestimento di zincatura in tutti gli acciai GA-IF e AHSS ha rivelato distinte tensioni residue di trazione, il che corrisponde alle previsioni teoriche. Gli acciai GA-AHSS hanno mostrato distinte tensioni residue di compressione sul lato acciaio del substrato, mentre per la maggior parte degli acciai GA-IF non si è evidenziata alcuna tensione residua di compressione sul lato acciaio del substrato. La mancanza di tensioni residue di compressione negli acciai GA-IF è probabilmente dovuta a un indebolimento dei bordi dei grani di acciaio per penetrazione di zinco liquido. E ciò è coerente con i risultati delle prove di taglio per trazione. Le due differenze principali nella struttura interfacciale tra acciai zincati GA-IF e AHSS sono (a) debolezza dei bordi dei grani dell'acciaio probabilmente a causa della penetrazione di Zn liquido al bordo, negli acciai GA-IF, e (b) interfaccia rivestimento/acciaio relativamente più liscia nell'acciaio GA-IF. Questi due fattori contribuiscono in modo significativo alla scarsa resistenza alla sfogliatura degli acciai GA-IF.